

MONOCRYSTALLINE SILICON PLASMA EXPANSION INDUCED BY MILLISECOND LASER

M. Guo^{a,b}, G. Jin^c, and X. Gao^c

UDC 533.9

Abstract: Ablation of monocrystalline silicon to atmospheric environment induced by a millisecond pulse of an Nd : YAG optical laser with a wavelength of 1064 nm is studied. Shadowgraphy is applied to study the process of monocrystalline silicon plasma expansion for the laser energy density of 955.4–2736.0 J/cm². It is shown that the outer boundary of the plasma plume diffuses outside with time. Plasma expansion occurs in both axial and radial directions, but the velocity of plasma expansion in the radial direction is smaller than in the axial direction. Two centerlines of the laser action are symmetric. The maximum expansion velocity of 162.1 m/s is reached with the laser energy density of 2376.0 J/cm², and a laser-supported combustion wave is generated in this case. In contrast to monocrystalline silicon under the action of a short-pulse laser, the millisecond laser action can make the plasma expansion velocity increase for the second time. A material splash can be observed from the expansion images in the case of a high laser energy density.

Keywords: millisecond laser, monocrystalline silicon, plasma, shadowgraphy.

DOI: 10.1134/S0021894418050243

INTRODUCTION

With the application of laser ablation to thin film deposition, micromachining, nanomaterial preparation, and analysis of chemical sample compositions [1–5], the phenomenon of the plasma induced by a laser has become a hot issue. Monocrystalline silicon affected by a high-power laser gives rise to mass transfer on the surface and to generation and expansion of a plasma plume. Detection methods for the expansion process mainly include optical interference, spectrum diagnosis, laser shadowgraphy/schlieren photography, etc. [6–9]. Shadowgraphy advantages are obvious: it offers visual and accurate information on plasma expansion in space and time. As the refractive index of the plasma has a specific spatial gradient perpendicular to the laser propagation direction, the probe beam is deflected by the plasma flow field and the shock wave front; as a result, the light intensity distribution of the charge coupled device (CCD), which converts the light intensity distribution into different shadow images, changes. The time-resolved shadow image can effectively represent the evolution of the plasma expansion boundary. Though the study of the characteristics of plasma expansion induced by a short-pulse laser has gained certain improvements, the main study objects tend to be metal target materials, while less attention is paid to monocrystalline silicon plasma induced by a millisecond laser.

Under the action of a millisecond pulse laser, there is a certain time delay between plasma activation and generation. Monocrystalline silicon is usually used as a window and substrate material; it is also an important

^aJilin Engineering Normal University, Institute for Interdisciplinary Quantum Information Technology, Changchun 130052, China; guoming1012@sina.com. ^bJilin Engineering Laboratory for Quantum Information Technology. ^cSchool of Science, Changchun University of Science and Technology, Changchun 130022, China; laser-cust@sina.com; lasergx@sina.com. Translated from *Prikladnaya Mekhanika i Tekhnicheskaya Fizika*, Vol. 59, No. 5, pp. 203–212, September–October, 2018. Original article submitted November 14, 2016; revision submitted March 15, 2018.

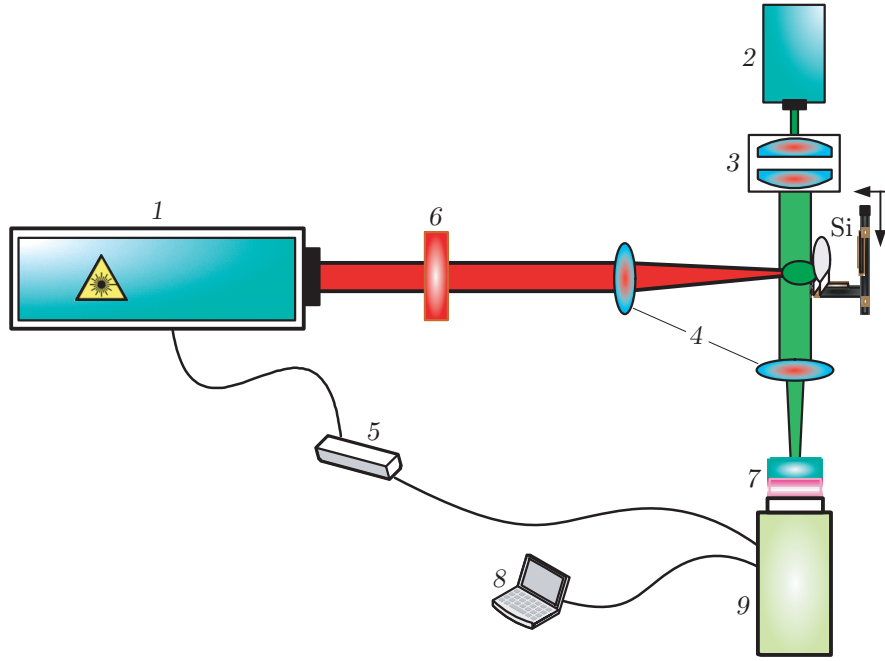


Fig. 1. Experimental facility: (1) Melar-100Ms laser system; (2) narrow linewidth diode laser; (3) beam expander; (4) lens; (5) pulse trigger; (6) attenuator; (7) attenuator filter; (8) computer; (9) V641 high-speed camera.

material for optoelectronic devices. The laser action on monocrystalline silicon may lead to various phenomena, including fusion, splashes, and other plasma phenomena. Hence, the rules and mechanisms of monocrystalline silicon plasma expansion induced by a laser pulse need to be further analyzed and studied.

This study makes use of high-speed cameras and other optical devices to investigate the process of monocrystalline silicon plasma expansion based on the laser shadow method. The effect of different laser energy densities on the plasma expansion velocity and distance is studied.

1. EXPERIMENTAL FACILITY

The experimental facility used to study plasma formation on the surface of monocrystalline silicon under a laser action is schematically shown in Fig. 1. The laser device used in this experiment is the Melar-100Nd: YAG pulse laser device with a single laser pulse output, which was produced by Beamtech Optronics Co., Ltd. Its reference data are the pulse width of 1 ms, pulse repetition frequency of 10 Hz, wavelength of 1064 nm, and maximum output energy of 100 J. The laser beam distribution is close to the Gaussian distribution. The beam diameter at the exit is 2 cm.

The energy adjustment system (consisting of a one-second wave plate and a polarizing film) and the plane-convex quartzose focusing lens with a focal length of 500 mm ensure vertical incidence of the laser beam onto the monocrystalline silicon sample surface.

The laser beam diameter is 2 mm after being focused. The monocrystalline silicon sample is clamped on a five-dimension translation stage. The shading imaging system consists of a high-speed camera, beam expander, and imaging lens. The probe beam after its expansion is captured by the imaging lens, and a high-speed CCD camera is used to obtain shadow maps. The wavelength of the semiconductor laser is 532 nm, and the linewidth is smaller than 0.7 nm. After ten-fold expansion by the expansion system, the beam is vertically incident onto the area of plasma expansion. After lens imaging, the beam energy is attenuated by the attenuator, and the interference filter filters the interference light. The changes in plasma expansion are observed by a V641 high-speed camera aligned at an angle of 90° with respect to the incident laser beam. The frame frequency of the high-speed camera is 10 000 fps. A digital delay pulse generator (type DG645, Stanford company) is triggered simultaneously with the laser. The single-sided polished (100) silicon wafer sample (4 mm thick and 25.4 mm in diameter) is set on an five-dimension

translation stage, which is put for 15 min into acetone and methanol for ultrasonic cleaning. The surface drops are purged with nitrogen. Then the sample is placed into a low-temperature drying box. The experiment is performed at room temperature in air at normal atmospheric pressure and relative humidity of 52%.

2. EXPERIMENT RESULTS AND ANALYSIS

Figure 2 shows the plasma plume photographs taken at different time instants. When ablated by a millisecond pulse laser, the generation of plasma takes place before the pulse end, in 0.1 ms after the beginning of the beam action. The monocrystalline silicon plasma plume expands outward with time. Its shape evolves from a regular semicircle, which experiences dispersion with time (see Fig. 2). The higher the laser energy density, the greater the distance of plasma outer boundary expansion. Finally, the generated plasma separates from monocrystalline silicon. For the laser energy density $W > 1981.4 \text{ J/cm}^2$, the plasma displays a plasma flash.

The action of the millisecond pulse laser takes a long time; it serves as a power source for plasma expansion. The laser energy favors accelerated expansion of the plasma in all directions.

For the laser energy density $W = 1582.4 \text{ J/cm}^2$, the plasma plume expands outward steadily and slowly within the pulse time. The outer boundary is regular and clear. After the pulse end, at $t = 1.1 \text{ ms}$, the outer boundary evolves into the shape of a mushroom cloud. At $t = 1.2 \text{ ms}$, the mushroom-shaped cloud almost separates from the monocrystalline silicon surface. This process is the free expansion process. For the laser energy density $W = 1981.4 \text{ J/cm}^2$, the ablated material amount obviously increases, and the splash occurs obviously faster than at $W = 1582.4 \text{ J/cm}^2$. Compared to the short-pulse laser action, obvious calefaction can be observed when monocrystalline silicon is affected by the millisecond laser. The expanding plasma plume transforms from a spheroidal shape to an almost ellipsoidal shape. The length of the major axis of the ellipsoid (axial direction) is 18.9 mm, and the length of the minor axis (radial direction) is about 10.1 mm. Two centerlines of the laser action are symmetric. The outer boundaries of the plasma plume become unclear. At $t = 0.7 \text{ ms}$, recombination promotes the emission of continuous radiation because of collisions between electrons and ions [10], and the plasma flash fills the entire plasma expansion area and its surrounding areas. For the laser energy density $W = 2736.0 \text{ J/cm}^2$, the outer boundaries of the plasma plume become unclear within 0.1 ms after the plasma flash appears due to the emission of monocrystalline silicon at high temperature and high pressure. The flash is the arc emitted by the plasma when it consumes energy during the process of its outward expansion. With an increase in the plasma expansion distance, the density of electrons and atoms in the plasma obviously decreases; the radiation of ionization and recombination become weaker. Some part of the subsequently added laser energy is inverse bremsstrahlung absorbed by the plasma. In contrast to the case with $W = 1981.4 \text{ J/cm}^2$, this serious flash appears 0.3 ms earlier in the case with $W = 2736.0 \text{ J/cm}^2$. The high-speed expansion of the plasma results in the emergence of obvious flash discontinuity surfaces. Some energy continues to act on the monocrystalline silicon surface through the heat conduction area. This energy acts together with intense plasma radiation on the surface, which activates silicon atoms. At $t = 1 \text{ ms}$, the plasma begins to splash violently and to emit outward in the shape of streamlines. With an increase in time, the plasma plume gradually evolves into the structure of a honeycomb and then disappears.

Figure 3 shows the plasma expansion distance and its expansion velocity under the action of the laser with the energy density $W = 1582.4 \text{ J/cm}^2$. It is seen that there are two time intervals where the silicon plasma expansion velocity increases. The expansion velocity instantly increases when acted by the laser and reaches its highest point $v_{\max} = 29.2 \text{ m/s}$ at $t = 0.2 \text{ ms}$. Then, the plasma expansion velocity decreases. At $t = 0.4 \text{ ms}$, the plasma expansion velocity increases again and reaches the second peak $v_{\max} = 18.8 \text{ m/s}$ at $t = 0.5 \text{ ms}$. Then the plasma expansion velocity starts to decrease again, and the changes in the expansion velocity gradually become unobtrusive after $t > 0.8 \text{ ms}$. The plasma is generated when silicon absorbs high laser energy. The plasma expansion velocity decreases since radiation and scattering deliver energy to external air.

The action of the millisecond laser takes a long time; hence, the subsequent laser energy absorbed during the process of plasma expansion is greater than the radiation energy. It promotes plasma activity and enhances the energy of the plasma group. Hence, the phenomenon of the repeated increase in the expansion velocity appears. The distance between the plasma expansion leading edge and the monocrystalline silicon surface increases with time and reaches the maximum value of 16.1 mm.

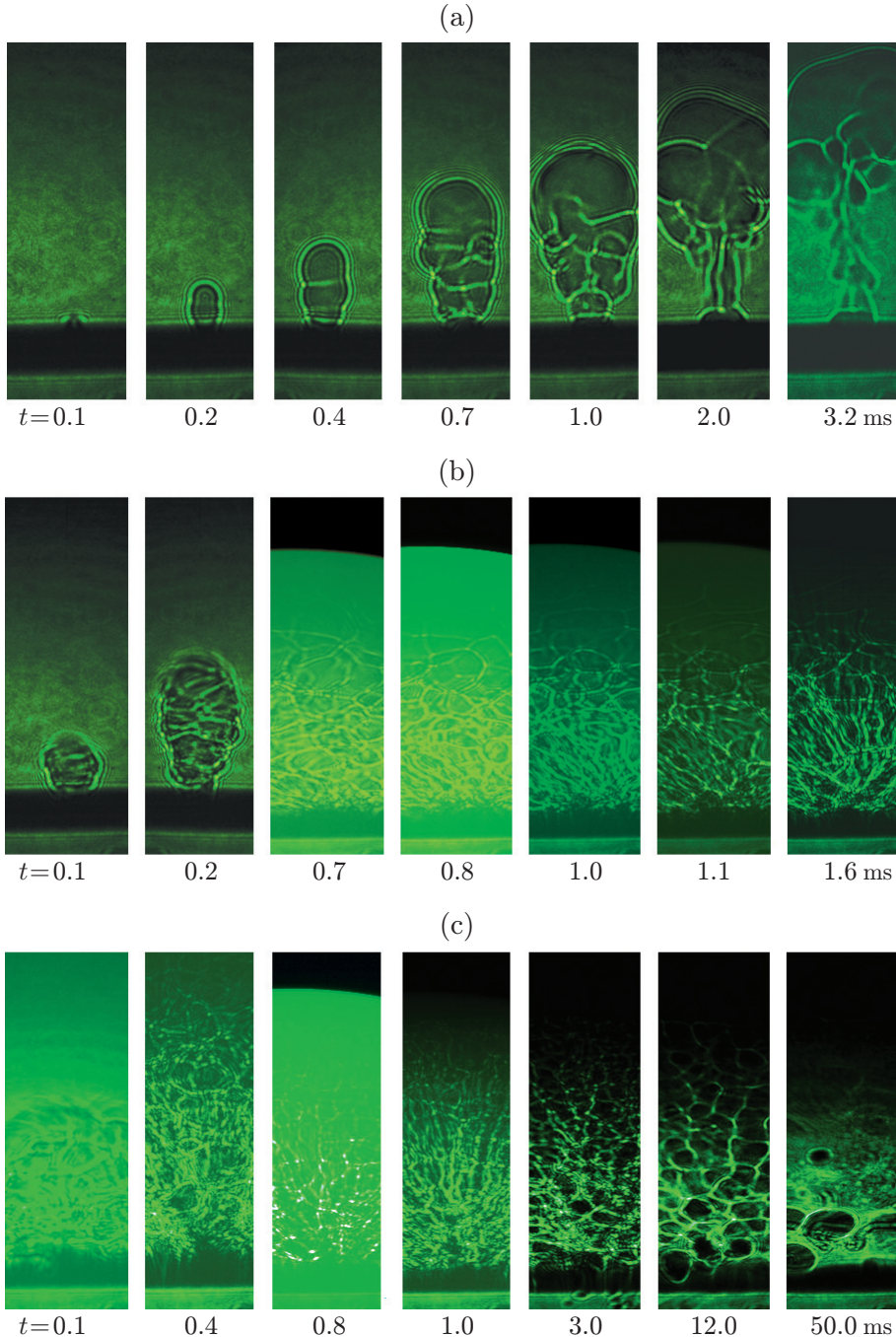


Fig. 2. Expansion of the monocrystalline silicon plasma plume at different time instants for $W = 1582.4$ (a), 1981.4 (b), and 2736.0 J/cm^2 (c).

Figure 4 shows the time evolution of the axial expansion distance of the monocrystalline silicon plasma. It can be learned from the figure that the plasma plume expansion distance increases quickly within $t = 0\text{--}0.3 \text{ ms}$, and then the increasing slows down, which illustrates that the plasma plume acceleration speed reaches the highest point when it is close to the monocrystalline silicon surface. The distance curves become steeper with an increase in the laser energy density, and the plasma expansion velocity increases. For the laser energy density $W < 1178.4 \text{ J/cm}^2$, the axial distance of plasma expansion is within 1 mm, and the plasma is close to the monocrystalline silicon surface. For the laser energy density between 1582.4 and 2486.4 J/cm^2 , the plasma expansion distances for different laser

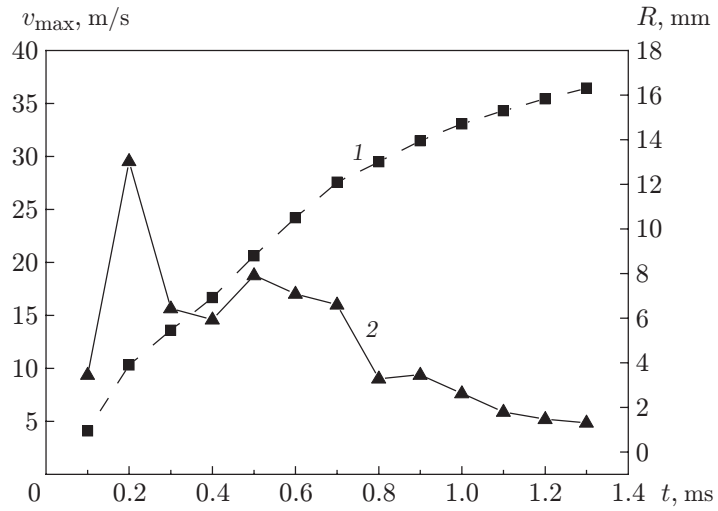


Fig. 3. Plasma expansion distance (1) and its expansion velocity (2) versus time for $W = 1582.4 \text{ J/cm}^2$.

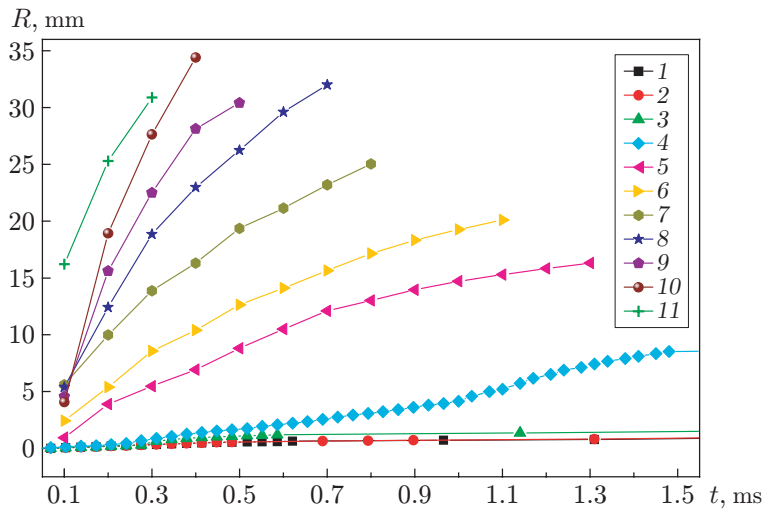


Fig. 4. Axial expansion distance of the monocrystalline silicon plasma plume versus time for different values of the energy density: $W = 955.4$ (1), 1050.9 (2), 1114.6 (3), 1273.9 (4), 1582.4 (5), 1806.4 (6), 1871.3 (7), 1981.4 (8), 2118.9 (9), 2486.4 (10), and 2736.0 J/cm^2 (11).

energy densities are within 5 mm at the beginning of the laser action (within 0.1 ms), and further variation is rather small. As the energy density is increased to $W = 2736.0 \text{ J/cm}^2$, the expansion distance reaches 15 mm at the time of 0.15 ms.

To solve the derivative based on the displacement curve of plasma plume expansion, we derive the expression for the plasma expansion velocity v :

$$v = \frac{dR}{dt}$$

(R is the expansion distance of the plasma plume and t is the time).

When the electrons of atoms are at the silicon surface, the latter is rapidly heated, which results in material ejection and generates the plasma composed of electrons, ions, and atoms. When the laser energy density reaches the threshold value of 955.4 J/cm^2 , plasma expansion occurs (Fig. 5). The plasma expansion velocity first increases and then decreases. The maximum velocity is smaller than 5 m/s. At the beginning of the laser action, the plasma

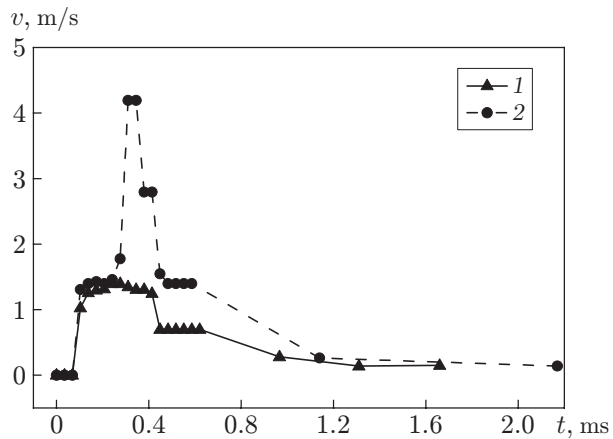


Fig. 5. Axial velocity of monocrystalline silicon plasma expansion versus time for small values of the laser energy density: $W = 955.4$ (1) and 1114.6 J/cm^2 (2).

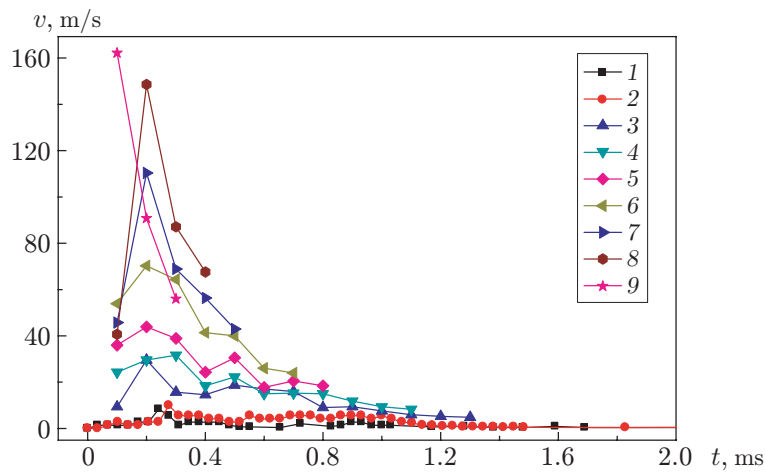


Fig. 6. Axial velocity of monocrystalline silicon plasma expansion versus time for large values of the laser energy density: $W = 1178.3$ (1), 1273.9 (2), 1582.4 (3), 1806.4 (4), 1871.3 (5), 1981.3 (6), 2118.9 (7), 2486.4 (8), and 2736.0 J/cm^2 (9).

volume expansion pressure is higher than the atmospheric pressure, and the expansion velocity rapidly increases. As the laser action and expansion are continued, the mean free path of particles elongates despite of the increase in the number of particles in the plasma. The probability of conversion of the internal energy of the plasma into the kinetic energy through particle collisions decreases. Thus, the motion of the outer boundary of the plasma gradually slows down. With an increase in the laser energy density, the plasma expansion velocity increases.

The evolution of the axial velocity of plasma expansion for high laser energy densities is illustrated in Fig. 6. With an increase in the laser energy density, the initial expansion velocity increases. The greater the energy density, the more obvious the velocity attenuation. For the laser energy density $W > 1178.3 \text{ J/cm}^2$, there are two time intervals where the plasma expansion velocity increases. In the case with the millisecond pulse laser, the influence of absorption of plasma drops on the laser energy cannot be neglected. During the millisecond laser action, its energy is absorbed by the expanding plasma, resulting in enhancement of the plasma expansion velocity. As the outer boundary of the plasma plume expands outward, the plasma volume becomes bigger, the mean free path of particles increases, and the probability of particle collisions decreases. At the same time, the heat exchange with external environment takes place; the plasma is rapidly cooled down, and its internal energy decreases. Hence, the kinetic energy of the plasma and its expansion velocity gradually decrease. The greater the laser energy density, the higher the expansion velocity peak. For the laser energy density $W = 1806.4 \text{ J/cm}^2$, the maximum plasma

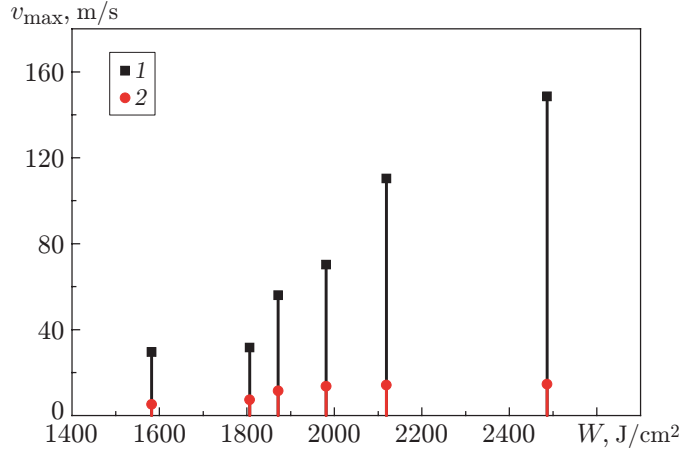


Fig. 7. Axial (1) and radial (2) maximum velocities of plasma expansion versus the laser energy density.

expansion velocity is 31.7 m/s. At $t > 0.4$ ms, the expansion velocity gently declines. The expansion velocity is about $v \approx 7$ m/s at $t = 0.9$ ms and then remains almost unchanged with time. At the laser energy density $W < 2486.4 \text{ J}/\text{cm}^2$, the plasma expansion velocity reaches its highest point $v = 148.6 \text{ m}/\text{s}$ at the time $t = 0.2$ ms. For $W = 2736.0 \text{ J}/\text{cm}^2$, the maximum expansion velocity is $v = 162.1 \text{ m}/\text{s}$. In this case, a laser-supported combustion wave is generated.

The maximum plasma expansion velocity v_{\max} is plotted in Fig. 7 as a function of the laser energy density. A large number of particles are spurt out in the axial direction, which is perpendicular to the monocrystalline silicon surface. A laser-supported absorption wave is formed under the action of the high energy density laser. The relationship between the plasma plume particle density and the absorption coefficient caused by inverse bremsstrahlung can be expressed as follows [11]:

$$k_a = \frac{3.69 \cdot 10^8 Z^3 n_i^2}{T_i^{1/2} \gamma_0^3} \left[1 - \exp \left(-\frac{h\gamma_0}{k_B T_i} \right) \right].$$

Here Z is the mean number of charged particles, n_i is the ion beam density, γ_0 is the incident beam frequency, T_i is the ion temperature, and $1 - \exp(-h\gamma_0/(k_B T_i))$ is the mean energy loss caused by stimulated radiation. In the radial direction, which is parallel to the monocrystalline silicon surface, most of the particles expand freely. Hence, the radial expansion velocity is smaller than the axial expansion velocity. The maximum velocity of plasma expansion increases with an increase in the laser energy density. For the laser density energy $W < 1806.4 \text{ J}/\text{cm}^2$, the plasma expansion velocity is low ($v = 30 \text{ m}/\text{s}$). When the laser energy density is in the interval $W = 1806.4\text{--}2118.9 \text{ J}/\text{cm}^2$, the plasma expansion velocity quickly increases and reaches $v = 56.1\text{--}110.4 \text{ m}/\text{s}$. With a continuing increase in the laser energy density, the expansion velocity acceleration slows down. For $W = 2736.0 \text{ J}/\text{cm}^2$, the plasma plume seriously absorbs subsequent high-density laser energy, and the plasma expansion velocity reaches its maximum value $v_{\max} = 162.1 \text{ m}/\text{s}$. The plasma moves forward with a subsonic speed. Due to the effect of thermal radiation, the air ahead shows the phenomena of ionization and calefaction, which leads to the formation of a laser-supported combustion wave. During the millisecond pulse laser action on monocrystalline silicon, the heating effect plays a key role. As the plasma electron density is rather low, the degree of ionization is weak; hence, a laser-supported detonation wave is not formed.

In addition to axial expansion of the monocrystalline silicon plasma, it also expands in the radial direction. Figure 8 shows the time evolution of the monocrystalline silicon plasma plume expansion distance in the radial direction. It can be seen that this parameter increases with time in an almost exponential form. With an increase in the laser energy density, the radial expansion distance increases. The initial radial size of the plasma plume is approximately 0.25 mm for all laser energy densities. The radial expansion distance is smaller than the axial expansion distance, which is caused by absorption of subsequent laser energy by the plasma during its expansion.

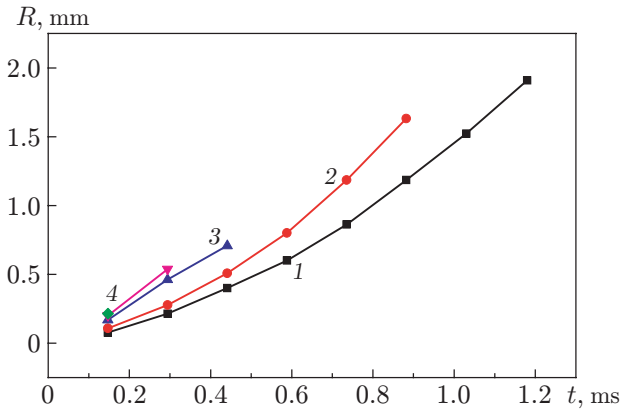


Fig. 8. Axial expansion distance of the monocrystalline silicon plasma plume versus time for different values of the laser energy density: $W = 1582.4$ (1), 1806.4 (2), 1871.3 (3), 1981.4 (4), and 2486.4 J/cm^2 (5).

CONCLUSIONS

The parameters of the plasma plume formed due to the action of a millisecond laser on monocrystalline silicon are studied. The thermal processes accompanying plasma formation, as well as the size and velocity of expansion of the plasma plume, are analyzed for different values of the laser energy density.

REFERENCES

1. S. Amoruso, R. Bruzzese, N. Spinelli, et al., "Generation of Silicon Nanoparticles Via Femtosecond Laser Ablation in Vacuum," *Appl. Phys. Lett.* **84**, 4502–4504 (2004).
2. Y. P. Li and Z. T. Liu, "Plasma Emission Diagnostics for the Optimization of Deposition Parameters in RF Magnetron Sputtering of GaP Film," *Acta Phys. Sinica* **58** (7), 5022–5028 (2009).
3. J. Perriere, C. Boulmer-Leborgne, R. Benzerga, and S. Tricot, "Nanoparticle Formation by Femtosecond Laser Ablation," *J. Phys. D: Appl. Phys.* **40** (22), 7069 (2007).
4. A. Y. Vorobyev, V. S. Makin, and C. L. Guo, "Brighter Light Sources from Black Metal: Significant Increase in Emission Efficiency of Incandescent Light Sources," *Phys. Rev. Lett.* **102** (23), 234–301 (2009).
5. T. H. Her, R. J. Finlay, C. Wu, et al., "Microstructuring of Silicon with Femtosecond Laser Pulses," *Appl. Phys. Lett.* **73** (12), 1673–1675 (1998).
6. J. Chen, J. G. Lunney, T. Lippert, et al., "Langmuir Probe Measurements and Mass Spectrometry of Plasma Plumes Generated by Laser Ablation of La_{0.4}Ca_{0.6}Mn_{0.3}," *J. Appl. Phys.* **116** (7), 073303 (2014).
7. A. Al Khawwam, C. Jama, P. Goudmand, et al., "Characterization of Carbon Nitride Layers Deposited by IR Laser Ablation of Graphite Target in a Remote Nitrogen Plasma Atmosphere: Nanoparticle Evidence," *Thin Solid Films* **408**, 15–25 (2002).
8. W. F. Wei, X. W. Li, J. Wu, et al., "Interferometric and Schlieren Characterization of the Plasmas and Shock Wave Dynamics during Laser-Triggered Discharge in Atmospheric Air," *Phys. Plasmas* **21**, 083112 (2014).
9. E. Nedanovska, G. Nersisyan, T. J. Morgan, et al., "Comparison of the Electron Density Measurements using Thomson Scattering and Emission Spectroscopy for Laser Induced Breakdown in One Atmosphere of Helium," *Appl. Phys. Lett.* **99** (26), 261504 (2011).
10. X. Gao, X. W. Song, H. Y. Tao, et al., "Optical Emission Spectra of Si Plasma Induced by Femtosecond Laser Pulse," *Acta Phys. Sinica* **60**, 025203 (2011).
11. Q. G. Zheng, *Interaction between Laser and Matter*, Ed. by Q. G. Zheng and J. H. Fu (Press of Huazhong Univ. of Sci. and Technol., Wuhan, 1996).